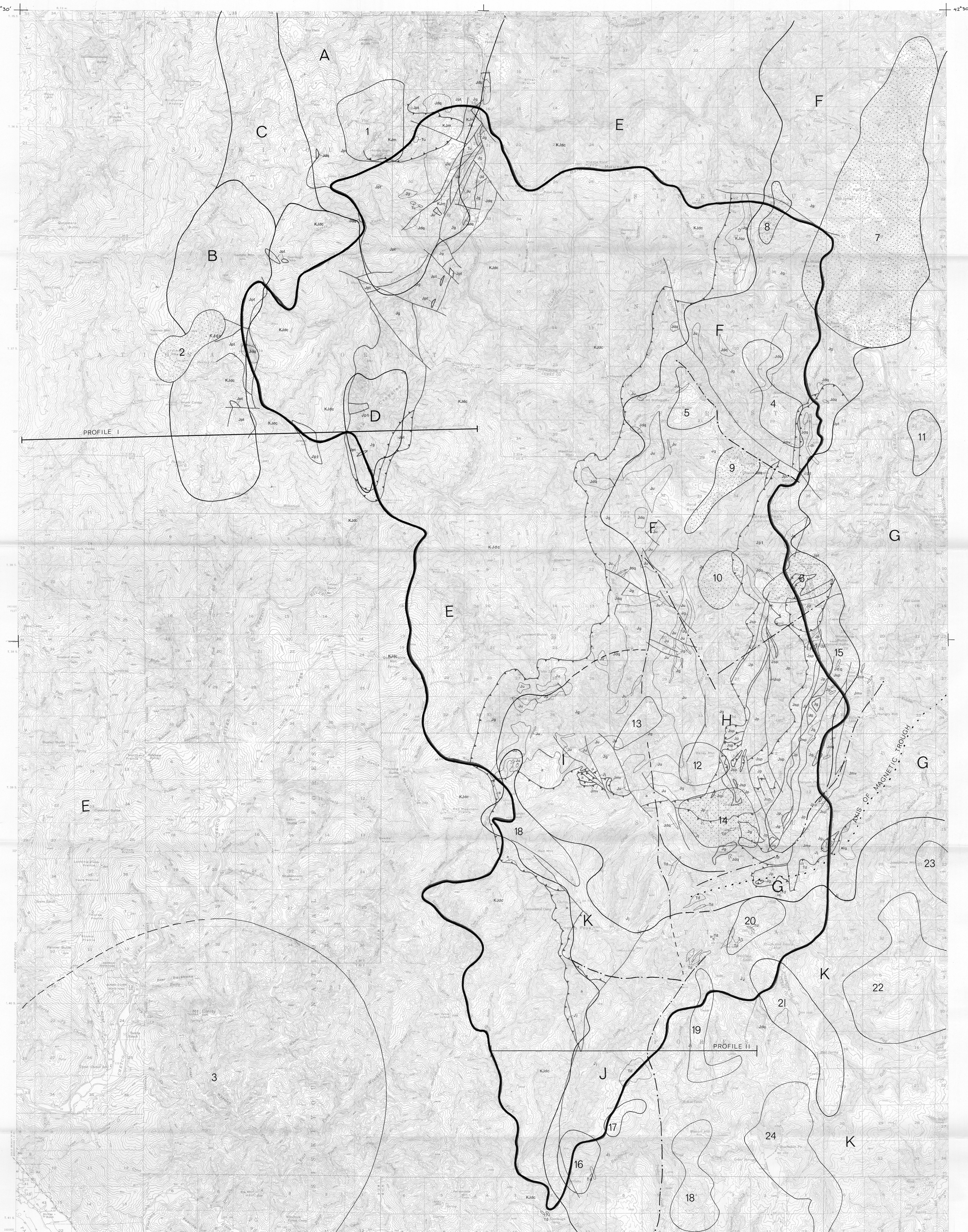

EXPLANATION

MAGNETIC BOUNDARIES–Dashed where uncertain. Letters refer to anomaly patterns; numbers to individual anomalies. Stipple areas are anomalies not caused by topography or mapped geology

MAGNETIC LINEATIONS–Dashed where uncertain. Also serves as boundary between anomaly patterns

PROFILE I — MAGNETIC PROFILE–See figure 1

CORRELATION AND DESCRIPTION OF GEOLOGIC MAP UNITS

TERTIARY

Tu — Umpqua Formation: Sandstone and shale

Td — Dacite dikes

CRETACEOUS AND JURASSIC

KJm — Myrtle Group (Lower Cretaceous and Upper Jurassic): Conglomerate, sandstone, and mudstone

KJqp — Quartz porphyry

KJdc — Dothan Formation (Cretaceous and Jurassic) and Colebrooke Schist (Upper Jurassic): Sandstone, shale, volcanic rocks, and schist

JURASSIC

Jmv — Metavolcanic rocks

Jp — Pyroxene-bearing metavolcanic rocks

Jdq, Jd, Jg, Ju — Intrusive igneous rocks: Jdq, diorite and quartz diorite; Jd, dike complex; Jg, gabbroic rocks; Ju, ultramafic rocks; predominantly metacumulate peridotite

JURASSIC AND JURASSIC OR OLDER

Jpt, Jj, Jsp, Jdi — Ultramafic rocks and dikes: Jpt, peridotite; Jj, Josephine Peridotite (Jurassic or older); Jsp, serpentinite; Jdi, diabase dikes

AGE UNKNOWN

a — Amphibolite

CONTACT--Approximately located

FAULT

THRUST FAULT--Sawteeth on upper plate

APPROXIMATE BOUNDARY OF KALMIOPSIS WILDERNESS

MAPS SHOWING AEROMAGNETIC DATA AND INTERPRETATION FOR THE KALMIOPSIS WILDERNESS, SOUTHWESTERN OREGON

By

Richard J. Blakely, Norman J Page, Floyd Gray, Lisa Senior, Holly F. Ryan

1983

STUDIES RELATED TO WILDERNESS

The Wilderness Act (Public Law 88-577, September 3, 1964) and related acts require the U.S. Geological Survey and the U.S. Bureau of Mines to survey certain areas on Federal lands to determine their mineral resource potential. Results must be made available to the public and submitted to the President and the Congress. This report presents the results of a geophysical survey of the Kalmiopsis Wilderness in the Siskiyou National Forest, Josephine and Curry Counties. Kalmiopsis Wilderness was established by Public Law 88-577.

INTRODUCTION

The distinctive magnetic properties of the major rock types in the Kalmiopsis Wilderness of southwestern Oregon facilitate interpretation of aeromagnetic data. The region is composed of tectonic slices of magnetic ultramafic, gabbroic, and other ophiolitic rocks faulted against the relatively nonmagnetic Dothan Formation, the equivalent of the Franciscan Complex of Western California. The sharp contacts between these rocks are manifested in the data by abrupt contrasts in the nature of the magnetic anomalies which provide insights into the structural relations of the major geologic elements.

Most individual anomalies in this area are caused by known geologic boundaries or topographic features; those that are not are of particular interest because they may reflect areas of increased or decreased magnetization associated with zones of mineralization.

MAGNETIC PROPERTIES

Table 1 shows the magnetic susceptibility of 90 samples from the Kalmiopsis Wilderness and adjacent terrane. The samples of ultramafic rock have been discussed elsewhere by Barnard and others (1981). Susceptibilities were determined on small cores drilled from unoriented hand samples using a susceptibility bridge. An unexpected result of these measurements is the relatively high susceptibility of the gabbros and metagabbros (arithmetic average = 8.51 ± 0.95 10^{-3} emu), which are even more magnetic than the ultramafic rocks (arithmetic average = 5.15 ± 0.74 10^{-3} emu). These magnetic gabbros also produce the most intense aeromagnetic anomalies.

AEROMAGNETIC DATA

The aeromagnetic data were compiled by mosaicking two published surveys along the north-south heavy dashed line shown in the map on sheet 1. The eastern survey is from Balsley and others (1960), hand contoured with a 50-gamma contour interval at a scale of 1:96,000 from data measured by the U.S. Geological Survey in 1950; it is not known what regional field was removed in this original compilation. The western survey (U.S. Geological Survey, 1979) was flown and compiled in 1978 by private contractor who subtracted from the data the International Geomagnetic Reference Field (IGRF) of 1975 updated to 1978. Both the western and the eastern surveys were flown along parallel east-west flight lines at a constant barometric altitude of 4500 ft (1372 m).

The western survey was recontoured by machine using contractor-supplied flight-line data. The eastern survey was hand digitized along flight lines using the data of Balsley and others (1960); a constant of 1750 gammas was subtracted from each value and the results were contoured by machine. The mosaiked compilation is at a scale of 1:62,500 and has a contour interval of 50 gammas. There are some apparent navigational errors in these data which appear as chevrons lineated in the east-west direction (for example, at lat 42°22' N. and long 123°57' W.). These chevrons do not represent lineated magnetic sources.

The aeromagnetic data show several magnetically distinct regions: (1) Anomalies caused by shallow magnetic sources are concentrated in the eastern third of the area. These correspond to the Josephine Peridotite and associated ophiolitic rocks. (2) West of these highly magnetic rocks are the mudstones, graywackes, and shales of the Dothan Formation. These relatively nonmagnetic materials underlie the areas of subdued anomalies that occupy most of the western part of the area. (3) Ultramafic rocks in the northwestern part of the area produce large amplitude anomalies with sharp boundaries.

INTERPRETATION

An interpretation of these magnetic anomaly patterns is shown in the map on sheet 2. A distinction is made between broad areas of anomaly "patterns", labeled with letters, and individual anomalies, labeled with numbers. In each case, the solid lines outline the approximate boundary of the source of the magnetic features. The following discussion describes individual anomalies and anomaly patterns starting with the northwest area of the map and progressing south.

Anomaly patterns A, B, and D are similar in nature and are probably caused by thin ultramafic sheets at or near the topographic surface. Anomaly pattern A, for example, is caused by peridotite tectonite. The eastern boundary of the tectonite is fragmented with blocks of gabbro, diorite, volcanic rocks, and the nonmagnetic Dothan Formation (Page and others, 1981), yet the eastern margin of anomaly pattern A is a broad linear gradient. It is possible that the eastern margin of the tectonite dips with a shallow angle to the east beneath these rocks. Within anomaly pattern A is a negative anomaly (anomaly 1) surrounded on the west, south, and east by positive anomalies. The southern boundary of anomaly 1 corresponds to the northern contact of the peridotite tectonite, where it dips under conglomerates of the Myrtle Group. The sharpness of this boundary, however, suggests that the tectonite is abruptly terminated against the conglomerate, in disagreement with the geologic evidence for a low-angle thrust (Coleman, 1972). Apparently the peridotite is very thin or nonmagnetic beneath this part of the Colebrooke Schist.

The sheet of peridotite causing anomaly pattern B seems from the magnetic data to connect at depth with the peridotite of anomaly pattern A. The approximate boundary of this deeper structure is shown by anomaly pattern C. Most of the anomaly maxima and minima within pattern B are probably caused by topographic perturbations and magnetization inhomogeneities within the ultramafic sheet. Anomaly 2, however, is caused by some feature, probably a fault, which extends across the western boundary of the ultramafic sheet and into the Colebrook Schist (Coleman, 1972).

Anomaly pattern D is underlain predominantly by gabbro and metagabbro. It was stated previously that gabbro and metagabbro of the Kalmiopsis Wilderness considered as a group, have higher susceptibilities than the average of all the ultramafic samples. However, the two specific samples of metagabbro from the area of anomaly pattern D (78KN045 and 78KZ059, table 1) have susceptibilities less than the average susceptibilities of either the gabbro and metagabbro or the ultramafic rocks. On the basis of these two samples, it appears that the mapped gabbro and metagabbro bodies are not the sources of anomaly pattern D. Geologic mapping shows that these gabbros and metagabbros are probably underlain at shallow depth by ultramafic rock which we propose as the source of anomaly pattern D. The magnetic data clearly define the lateral extent of this shallow ultramafic sheet and show that it is detached from the sources of patterns A and B.

A magnetic model for these ultramafic sheets is shown in figure 1 (sheet 2), using the data along profile I (sheet 2). Assumptions implicit in this model are: (1) The bodies are assumed to continue uniformly to great distances in the directions perpendicular to profile I, and (2) the magnetization is assumed to be uniform and parallel to the Earth's magnetic field throughout each body. The first assumption ignores the three-dimensional shape of the ultramafic sheets, but introduces only minor errors because the major anomaly boundaries are linear for several kilometers in the north-south direction. The second assumption is more tenuous because it asserts that remanent magnetization is small compared to the susceptibility, a requirement that ultramafic rocks may not satisfy.

The calculated profile is a close approximation to the observed profile, especially considering the simplicity of the model. Errors caused by our assumptions would not alter the important conclusions: (1) The sources of anomalies B and D are thin sheets of magnetic material located near the Earth's surface, probably klippen of ultramafic rocks. (2) The sheet causing anomaly pattern B is not necessarily connected to the sheet causing pattern D. (3) The klippe of ultramafic rock that forms the peak of Green Craggie (located along profile I midway between patterns B and D) is either nonmagnetic or extremely thin.

These ultramafic sheets are surrounded by the Dothan Formation (anomaly pattern E). These mudstones, graywackes, and shales have very low magnetizations and produce a generally featureless aeromagnetic pattern. However, a very broad, circular anomaly (3) lies in the southwestern corner of the area. The source of this anomaly is deep and may be a buried pluton. A Tertiary stock is exposed at Mount Emily 1.6 mi (2.5 km) north of the center of this anomaly, and although Mount Emily itself produces no anomaly, it may be geologically related to the deep source of anomaly 3. Rock geochemistry (Carlson and others, 1981) identifies a suite of geochemical anomalies in the Tertiary dikes east of anomaly 3 that seem to be related to Mount Emily. Apparently, the plutonic event that produced Mount Emily was more widespread than suggested by exposures at Mount Emily.

The eastern third of the aeromagnetic map is characterized by a region of short-wavelength anomalies caused by peridotites, gabbros, and volcanic rocks. A thrust fault, here informally called the Valen Lake thrust after Ramp (1975), forms the boundary of these rocks with the nonmagnetic Dothan Formation; this fault is clearly expressed in the magnetic data as the eastern edge of pattern E. At about lat 42°12' N. an east-west thrust fault, called the Madstone Cabin thrust by Ramp (1975), separates the Josephine Peridotite to the south from predominantly gabbroic and ultramafic cumulate to the north. South of the Madstone Cabin thrust, the east edge of pattern E is nearly coincident with the Valen Lake thrust. North of this point, however, the magnetic boundary is displaced an average of .6 mi (1 km) to the east of the Valen Lake thrust. The reasons for this offset are not clear. Perhaps the west edges of the gabbros are very thin, but abruptly thicken at the magnetic boundary, or possibly the gabbros are underlain by some other magnetic material. We prefer the latter interpretation on the basis of the geologic evidence (Page and others, 1981) and our interpretation of anomaly patterns A, B, and D. It is possible that much of the terrane north of the Madstone Cabin thrust is underlain by unconnected slivers of serpentinized ultramafic rocks.

Anomaly pattern F overlies terrane largely composed of cumulate gabbro, metagabbro, and peridotite, but the pattern of anomalies has little relation to mapped contacts between these rocks. Apparently, either the magnetic properties of the rocks in area F do not correlate with rock type or the rocks exposed at the surface do not extend to significant depths. Some of the individual anomalies within pattern F correspond to topographic highs. Anomaly 4 is situated over Nome Peak, composed of hornblende gabbro, and anomaly 5 is over Granite Butte, a cumulate gabbro body. Anomaly 6 is over peridotite tectonite that includes local concentrations of dunite, and the high degree of serpentinization in this area may explain this magnetic feature.

Several anomalies in the cumulate-gabbro terrane are not so easily explained, however. Anomaly 7, for example, has the largest amplitude of any in the entire area yet is not related to any major topographic feature. Likewise, anomalies 8, 9, and 10 are not related to any large topographic or geologic feature. The susceptibility measurements of table 1 suggest that exposed gabbros are sufficiently magnetic to produce the anomalies. In similar terrane to the west, however, anomaly patterns A, B, and D are caused by slivers of serpentinized ultramafic rock, in some cases lying under relatively nonmagnetic gabbro. It is possible, therefore, that the high-amplitude anomalies within pattern F have a similar origin: unexposed, disconnected wedges of serpentinized ultramafic rock.

A ground magnetometer survey was conducted by Gray (1980) in the area underlying anomaly pattern F between Tincup Peak and Gold Basin. Traverses were made across a low-grade cumulus magnetite ore deposit located within a partially serpentinized ultramafic body bounded on the west and east by gabbro. The data outline a northeast-trending (N. 43° E.), 490 ft (150 m) wide, positive anomaly that coincides closely with the major concentration of cumulus magnetite in the ultramafic rock. The anomaly is asymmetric with a steep gradient to the northwest where ultramafic rock is in steep contact with gabbro and with a more gentle gradient to the southeast where the ultramafic rock dips beneath cumulus gabbro along a low-angle contact, interpreted as a thrust fault by Gray (1980).

The northeast-trending unit of ultramafic rock containing the magnetite deposit does not produce an aeromagnetic anomaly, suggesting that it is a rather thin (<3300 ft (1000 m)) sheet of magnetic material. However, a northeast-trending, high-amplitude feature (anomaly 9) just east of Tincup Peak, in the Gold Basin area, suggests that the magnetite-bearing ultramafic rocks of Tincup Peak may extend eastward beneath the sheet of gabbroic rock.

Anomaly pattern G, is a long magnetic trough with very broad gradients. The trough is not caused by a topographic depression. Fiddler Mountain, for example, is within pattern G and produces no individual anomaly. Pattern G is situated over a terrane that consists predominantly of metavolcanic rocks interbedded with shale. These rocks typically have low magnetization which explains the troughlike feature. Part of the axis of the trough overlies the Madstone Cabin thrust, which here forms the boundary between these metavolcanic rocks and the Josephine Peridotite. At its southwest end, the trough crosses into the area of the peridotite, a configuration which suggests that the volcanic rocks extend to great depths in this area and probably form a wedge beneath the overthrust Josephine Peridotite.

The only individual anomaly of note within pattern G is anomaly 11. It occurs over a moderate topographic high, but other major topographic features (e.g., the Illinois River and Fiddler Mountain) in this metavolcanic terrane produce no magnetic anomalies. The anomaly may be the result of mineralization, although no geochemical anomalies were detected (Carlson and others, 1981).

Anomaly pattern H is separated from F by two abrupt magnetic gradients. The gradient that trends northwest corresponds to a series of northwest-trending faults. The northeast-trending gradient may be caused by the complex arrangement of northeast-trending slices of volcanic and ultramafic rocks. Pattern H is over a fragmented terrane of metagabbro, peridotite tectonite, serpentinite, and metavolcanic rocks. All three individual anomalies in pattern H are at least partly caused by topography. Anomaly 12 is situated over metagabbro of Bailey Mountain. Anomaly 13 is over that part of a long northeast-trending ridge that is composed of hornblende gabbro. The fact that other parts of the ridge do not generate anomalies indicates that the gabbro probably contains a high concentration of magnetite. Anomaly 14, a minimum, is over a mild topographic depression caused by the Little Chetco River in the Emily Cabin area. It also overlies part of the Madstone Cabin thrust fault between the peridotite tectonite unit of Page and others (1981) to the north and the Josephine Peridotite to the south. The magnetic minimum may represent an area of alteration associated with known volcanogenic massive sulfide occurrences (Ramp, 1975) within the metavolcanic rocks. Anomaly 15 lies over a north-trending ridge which includes Whetstone Butte and Canyon Peak. Most of this ridge is metavolcanic rock containing slivers of serpentinite and gabbro.

Anomaly pattern I is a magnetically subdued region that spans the Madstone Cabin thrust. There is no magnetic expression of this thrust within pattern I. Indeed, the lack of magnetic expression throughout pattern I was not expected. The gabbros and peridotites in this region must either be very thin or have very low magnetizations. Vulcan Peak within pattern I has many exposures of unaltered peridotite. If Vulcan Peak is representative of all the peridotite of pattern I, then the subdued anomaly pattern may reflect low concentrations of magnetite (a product of serpentinization of ultramafic rocks).

Anomaly pattern J is another region of subdued magnetic anomalies, but it has an abrupt boundary with the Dothan Formation along its western edge. Its eastern boundary with pattern K is also an abrupt linear anomaly that we believe is a major tectonic feature not previously recognized. This feature extends north to the boundary between patterns I and H, where it parallels the northwest-trending gradient between patterns F and H discussed previously, and extends south to a south-trending fault mapped by Wells and others (1949) at lat 42°00' N.

A magnetic model was derived from the data along profile II in order to help define this tectonic boundary (fig. 2). The same assumptions described earlier for figure 1 are implicit in this model, but conclusions from figure 2 are more tenuous because most individual anomalies do not trend north-south, perpendicular to the profile. With this qualification, figure 2 shows that the source of anomaly pattern J can be modeled as a very thin veneer of peridotite which abruptly thickens at the western edge of anomaly pattern K. We suggest that the sources of patterns J and K are separate pieces of the sheet composed of the Josephine Peridotite separated by a north-south discontinuity.

Anomalies 16 and 17 within pattern J are a magnetic high and low, respectively, over a northeast-trending ridge along the wilderness boundary. This ridge is composed of the Josephine Peridotite and the anomalies probably reflect varying degrees of serpentinization.

Anomaly pattern K covers a large area of the Josephine Peridotite. Anomaly 18 lies over the ridge that includes Vulcan Peak and Red Mountain. The arm of pattern K that extends south from this anomaly is parallel to an exposed amphibolite body. The anomaly is sufficiently offset from the amphibolite unit to indicate this unit is not significantly magnetic.

Other individual anomalies in pattern K (19–24) are not related to topographic features within the peridotite and probably reflect zones of more intense serpentinization. Anomaly 24 is an especially interesting negative anomaly that includes a topographic high, Buckskin Peak. Buckskin Peak may be an area of very low serpentinization, or it may consist of rocks with reversed remanent magnetization (Blakely and Page, 1980). The axis of anomaly 21 is located roughly 2 mi (3 km) northeast of the axis of a granodiorite pluton (Wells and others, 1949) within the Josephine Peridotite. This offset is too great for the anomaly to be directly caused by the pluton.

CONCLUSIONS

Magnetic minerals of importance to geologic studies are of two groups: iron-titanium oxides (magnetite, hematite, maghemite) and iron sulfides (pyrrhotite). In general, mafic igneous rocks have greater concentrations of these oxides and sulfides than silicic rocks. Sedimentary rocks can become important magnetic sources due to the mobilization of sulfides during lithification and metamorphism.

Most of the anomalies shown on sheet 2 can be explained by topograhic features or known geologic contacts. Those anomalies which are not so simply explained are noted on the map by a stipple pattern and have been discussed individually above. Iron-titanium oxides or iron sulfides may concentrate during the formation of ore bodies, or they may be destroyed by hydrothermal alteration so that zones that have higher or lower magnetizations than surrounding areas may reflect sites of mineralization. Hence, the stipple patterns indicate areas that should be considered in a mineral assessment.

REFERENCES

Balsley, J. R., Bromery, R. W., Remington, E. W., and others, 1960, Aeromagnetic map of the Kerby and part of the Grants Pass quadrangles, Josephine and Curry Counties, Oregon: U.S. Geological Survey Geophysical Investigations Map, GP-197, scale 1:96000.

Barnard, J. B., Page, N. J, Blakely, R. J., Ziemianski, W. P., Banister, C. A., and Giusso, J. R., 1981, Map showing distribution of serpentine minerals, density, and magnetic susceptibility of rocks from the Kalmiopsis Wilderness, Southwestern Oregon: U.S. Geological Survey Miscellaneous Field Studies Map MF-1240-B, scale 1:62,500.

Blakely, R. J., and Page, N. J, 1980, Interpretation of aeromagnetic data over the Josephine peridotite, southwestern Oregon, and implications for marine magnetic anomalies [abs.]: American Geophysical Union Transactions, v. 61, p. 943.

Carlson, C. A., Page, N. J, Grimes, D. J., and Leinz, R. W., 1981, Geochemical characteristics of rock samples from the Kalmiopsis Wilderness, Southwestern Oregon: U.S. Geological Survey Miscellaneous Field Studies Map MF-1240-C, scale 1:62,500.

Coleman, R. G., 1972, The Colebrooks Schist of southwestern Oregon and its relation to the tectonic evolution of the region: U.S. Geological Survey Bulletin 1339, 61 p.

Gray, Floyd, 1980, Geology of the igneous complex at Tincup Peak, Kalmiopsis Wilderness Area, southwestern Oregon: U.S. Geological Survey Open-File Report 80-1243, 65 p.

Page, N. J, Gray, F., Cannon, J. K., Foose, M. P., Lipin, B., Moring, B. C., Nicholson, S. W., Sawlin, M. G., Till, A., and Ziemianski, W. P., 1981, Geologic map of the Kalmiopsis Wilderness, Oregon: U.S. Geological Survey Miscellaneous Field Studies Map MF-1240-A, scale 1:62,500.

Ramp, L., 1975, Geology and mineral resources of the upper Chetco drainage area, Oregon, including the Kalmiopsis Wilderness and Big Craggies Botanical areas: Oregon Department of Geology and Mineral Industries Bulletin 88, 47 p.

U.S. Geological Survey, 1979, Aeromagnetic map of the Medford area, Oregon: U.S. Geological Survey Open-File Report 79-1195, scale 1:250,000.

Wells, F. G., Hotz, P. E., and Cater, F. W., Jr., 1949, Preliminary description of the geology of the Kerby quadrangle, Oregon: Oregon Department of Geology and Mineral Industries Bulletin 40, 23 p.

Table 1. Magnetic susceptibility of rock samples from the Kalmiopsis Wilderness and surrounding area.

Sample	Latitude	Longitude	Susceptibility (10^{-3} emu)	Rock type
76KG021	42.16602	123.92350	0.18	Peridotite
76KP004	42.14943	123.89178	5.55	"
76KP008	42.14509	123.90593	1.02	"
76KP009	42.13474	123.91646	0.25	"
76KP010	42.14133	123.85532	2.16	"
76KP012	42.14560	123.85113	1.01	"
76KP022	42.12226	123.83977	3.02	"
76KP023	42.10333	123.83051	1.23	"
76KP024	42.08998	123.82014	0.64	"
76KP027	42.08158	123.82439	0.40	"
76KP028	42.15233	123.84213	2.68	"
76KP036	42.16694	123.78786	0.51	"
76KP042	42.17403	123.84836	0.65	"
76KP081	42.19477	123.85161	1.41	"
76KP089	42.18075	123.89516	2.48	"
76KP110	42.18089	123.93329	0.26	"
76KP111	42.17678	123.94105	2.71	"
76KP117	42.17767	123.92003	0.33	"
76KS084	42.18950	123.93824	3.51	"
76KT004	42.17664	123.94710	2.73	"
76KT073	42.18861	123.86801	0.30	"
78KG133	42.43238	124.08274	1.71	"
78KJ005	42.42027	124.02853	7.34	"
78KJ030	42.05852	123.90819	2.01	"
78KP013	42.07602	123.92640	1.46	"
78KP018	42.08344	123.94425	0.77	"
78KW068	42.26267	123.81476	4.88	"
78KZ024	42.18262	123.98519	0.34	"
78KZ027	42.17455	123.98134	0.31	"
78KJ003	42.43256	124.02484	2.44	Harzburgite
76KP078	42.19141	123.86779	9.82	Wehrlite
76KP040	42.18405	123.83348	1.50	Pyroxenite
76KP054	42.22590	123.88511	2.06	"
76KP061	42.21577	123.89731	5.57	"
76KP195	42.22768	123.91646	3.81	"
78KG134	42.43220	124.08260	0.16	"
78KG209	42.21244	123.91957	4.50	"
78KG216	42.30996	123.91061	34.30	"
78KL150	42.40069	124.10998	0.05	"
78KJ015	42.42721	124.00839	0.21	Metapyroxenite
78KZ058	42.34049	124.05721	4.71	"
76KP032	42.16534	123.81117	2.67	Dunite
76KP060	42.21840	123.89506	5.85	"
76KP098	42.20129	123.90553	3.94	"
78KP001	42.10307	123.88279	0.56	"
78KZ031	42.16896	123.97121	0.99	"
76KP094	42.19176	123.90367	0.11	Chromite
76KP134	42.23719	123.81394	7.72	Serpentinite
78KL213	42.03847	123.94810	5.49	"
78KW069	42.26989	123.82560	8.06	"
76KT078	42.27941	123.87173	9.79	Gabbro
78KC040	42.39832	123.86238	6.86	"
78KC084	42.33482	123.85117	9.66	"
78KC085	42.35074	123.86563	15.60	"
78KC086	42.35790	123.87177	14.10	"
78KF108	42.34757	123.84421	5.84	"
78KG047	42.38389	123.92321	4.90	"
78KG109	42.34344	123.87286	12.00	"
78KL082	42.40072	123.85430	10.90	"
78KN045	42.35855	124.06157	0.17	"
78KW023	42.34972	123.84644	10.90	"
78KW028	42.36820	123.85380	14.70	"
78KW029	42.37169	123.85844	16.20	"
78KW045	42.37872	123.84612	14.60	"
79GA42N	42.54994	123.68085	10.80	"
76KP067	42.18920	123.88560	0.05	Metagabbro
76KP076	42.18214	123.86579	9.42	"
76KP106	42.19165	123.91739	1.38	"
76KP255	42.23978	123.92415	1.06	"
78KB084	42.35744	123.90810	3.60	"
78KB087	42.36271	123.91309	7.88	"
78KB107	42.11503	123.84316	16.60	"
78KG166	42.38902	124.03866	4.25	"
78KJ007	42.42138	124.01566	4.93	"
78KN036	42.42312	124.01241	8.59	"
78KP031	42.41674	124.01671	4.46	"
78KP035	42.40905	124.01418	9.09	"
78KW036	42.38738	123.85598	15.10	"
78KZ059	42.34312	124.05544	3.24	"
78KP008	42.06784	123.91321	0.02	Diorite
76KP297	42.24011	123.93930	2.64	Quartz diorite
79GA87N	42.58149	123.67681	13.20	"
79GA90N	42.68253	123.62072	3.31	"
79PE75N	42.49497	123.75832	8.01	"
79PE140N	42.49448	123.82822	4.06	"
79PE148N	42.44580	123.83609	9.79	"
78KW039	42.38932	123.84974	3.16	Hornblende diorite
76KP011	42.14133	123.85532	3.85	Amphibolite
78KL148	42.40850	124.11260	0.02	Graywacke
78KP009	42.08451	123.91321	0.16	Porphyry

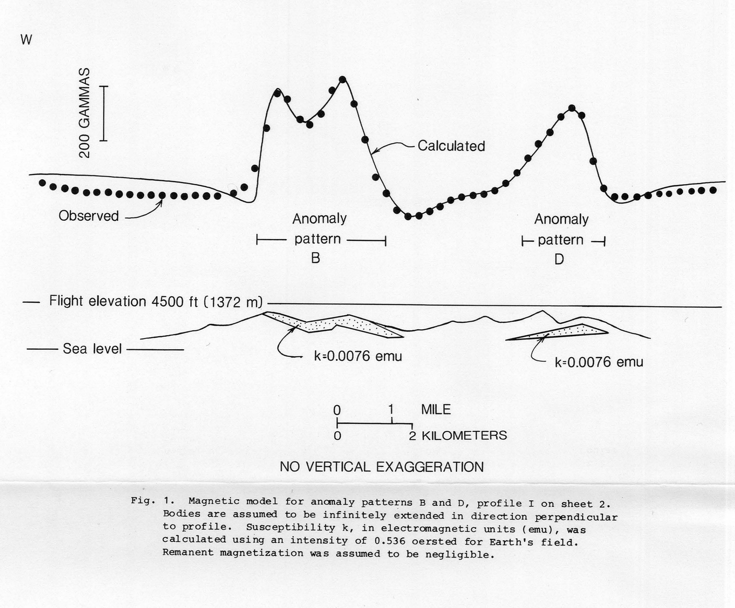

Fig. 1. Magnetic model for anomaly patterns B and D, profile I on sheet 2. Bodies are assumed to be infinitely extended in direction perpendicular to profile. Susceptibility k, in electromagnetic units (emu), was calculated using an intensity of 0.536 oersted for Earth's field. Remanent magnetization was assumed to be negligible.

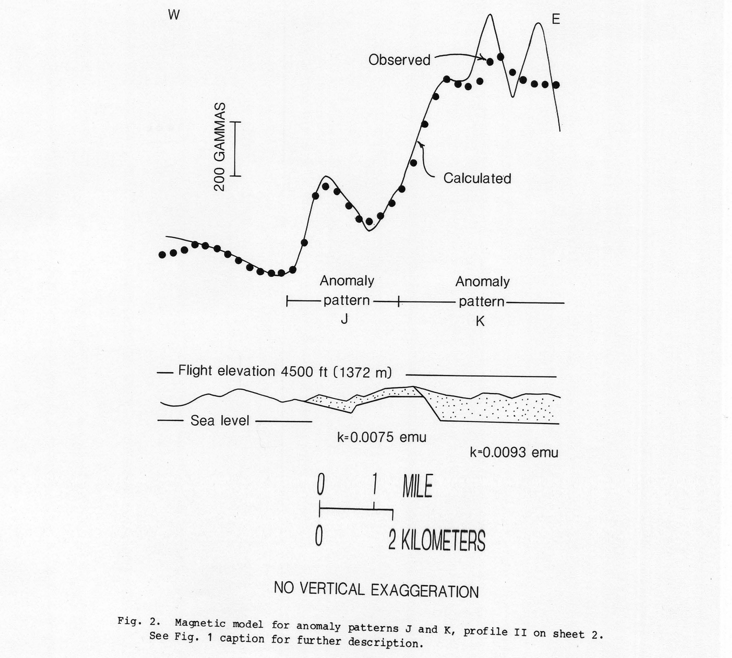

Fig. 2. Magnetic model for anomaly patterns J and K, profile II on sheet 2. See Fig. 1 caption for further description.